Polymer Chemistry

Fluorinated Zwitterionic Polymers as Dynamic Surface Coatings

Journal:	*Polymer Chemistry*
Manuscript ID	PY-COM-09-2022-001197.R1
Article Type:	Communication
Date Submitted by the Author:	06-Nov-2022
Complete List of Authors:	Zhou, Le; University of Massachusetts-Amherst, Polymer Science and Engineering Yang, Zhefei; University of Massachusetts-Amherst, Polymer Science and Engineering Pagaduan, James Nicolas; University of Massachusetts-Amherst, Polymer Science and Engineering Emrick, Todd; University of Massachusetts-Amherst, Polymer Science and Engineering

ARTICLE

Fluorinated Zwitterionic Polymers as Dynamic Surface Coatings

Le Zhou,†[a] Zhefei Yang,†[a] James Nicolas Pagaduan,[a] Todd Emrick*[a]

Received 00th January 20xx,
Accepted 00th January 20xx

DOI: 10.1039/x0xx00000x

Polymer modification of metallic and inorganic substrates represents an important strategy to determine key surface properties, including wetting, adhesion, and biomolecular interactions. The versatility of polymer chemistry and surface-grafting techniques has enabled the preparation of a wide array of functional surfaces that exhibit enhanced utility relative to pristine, unmodified materials. However, despite recent progress, discovering new polymer compositions for surface modification is essential to address ongoing challenges related to surface properties and functional interfaces. This manuscript describes surface grafting using fluorinated polymer zwitterions by surface-initiated atom transfer radical polymerization (SI-ATRP). The resultant polymer-coated substrates exhibited wetting characteristics intermediate between those of zwitterionic and fluorinated polymer brushes, with unusually large contact angle hysteresis values that are indicative of polymer response to the contacting fluid. Notably, surfaces functionalized with fluorinated polymer zwitterions exhibited impressive resistance to protein fouling with bovine serum albumin and lysozyme.

Introduction

The rapidly growing library of functional polymers, in combination with advances in controlled polymerization techniques, represents an exceptionally useful platform for controlling surface chemistry and topology.[1–3] For example, surfaces characterized by “extreme wettability”, i.e., that are superhydrophilic or superhydrophobic, have interesting and useful properties ranging from antifogging to self-cleaning to controlled adhesion.[4–6] Functionalized surfaces equipped for selective molecular interactions are useful in separations and sensing.[7,8] Surfaces may also be engineered to mimic the wettability of exquisite structures in Nature, such as lotus leaves (superhydrophobic)[9] or rose petals (large contact angle hysteresis).[10] Overall, the ability of polymers to bridge the interface between a substrate and its surrounding environment effectively tailors surface properties (wettability, adhesion, electronics, etc.) and provides a route to improved medical devices, implants, biosensors, and electronic materials.[11–13]

Synthetic polymers are prime candidates for use as fouling resistant coatings, especially hydrophilic polymers, such as poly(ethylene oxide) (PEO) and polymer zwitterions.[14] Polymer zwitterions are notable for their particularly outstanding performance, as the surface hydration promoted by their inner-salt structure masks nonpolar biomolecule-surface interactions.[15] To date, phosphorylcholine (PC), sulfobetaine (SB), and carboxybetaine (CB) represent the most frequently utilized chemistry for polymer surface modification.[16] Other approaches to achieve antifouling properties involve coatings of fluoropolymers and silicone elastomers, each contributing low surface energy that weakens interactions with potential foulants, enabling foulant release.[17,18] Despite this progress on hydrophilic and fluorophilic surface modifications, continued progress in this field requires the discovery of new materials interfaces capable of responding to different environmental conditions and which contribute both hydrophilic and fluorinated characteristics.

Recent studies have examined the combination of hydrophilic and fluorinated groups within the same chemical structure. For example, Xu, *et al.* coated surfaces with polymers containing both trifluoromethyl and PEG side chains to afford synergistic non-fouling/fouling release behavior with proteins.[19] In some cases, modifying surfaces with amphiphilic polymers may enhance antifouling performance, and as such this approach is being examined in marine coatings and medical implants.[20,21] Our group recently reported the synthesis of polymer zwitterions that embed fluorinated groups directly into choline phosphate sub-units, giving fluorinated choline phosphates (FCPs). In a preliminary protein fouling experiment, FCP coatings appeared to provide significant non-fouling properties; moreover, the non-aqueous solubility of the coating allowed it to remain on the substrate in water.[22] In this work, we seek deeper appreciation of the impact of FCPs on surface properties. As illustrated in **Figure 1**, using surface-initiated atom transfer radical polymerization (SI-ATRP), Au substrates were modified with polymer zwitterions, fluorinated polymers, or FCPs. The unique zwitterion/fluorocarbon combination of FCPs afforded surfaces with distinctly different properties relative to PMPC or fluoropolymer-grafting, including notably high contact angle hysteresis values suggestive of dynamic surface rearrangement. Using surface plasmon resonance (SPR) techniques, BSA and lysozyme adsorption was examined, with

[a] *Polymer Science and Engineering Department, Conte Center for Polymer Research, University of Massachusetts, 120 Governors Drive, Amherst, MA 01003, USA. E-mail: tsemrick@mail.pse.umass.edu.*
† Le Zhou and Zhefei Yang contributed equally to this work.
Electronic Supplementary Information (ESI) available: [details of any supplementary information available should be included here]. See DOI: 10.1039/x0xx00000x

results indicating significant protein resistance owing to FCP grafting. Overall, to our knowledge this paper describes the first example of covalent surface grafting using FCPs and demonstrates the potential of these functional substrates as antifouling materials.

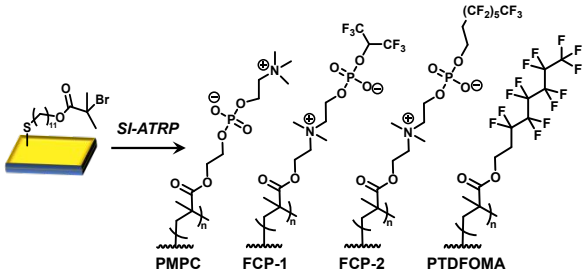

Figure. 1. Schematic representation of **PMPC**, **FCP-1**, **FCP-2** and **PTDFOMA**-grafted Au substrates by SI-ATRP.

Results and discussion

Au-coated Si wafers were functionalized suitably for ATRP, using literature preparations,[23] and employed for SI-grafting of zwitterionic, fluorinated, and "fluorozwitterionic" FCP polymers, as shown in **Figure 1**.[22] SI-ATRP was performed by placing the substrates in 7 mL vials containing 0.3-0.5 M monomer solutions in trifluoroethanol (TFE) at room temperature for 1-4 hrs, with CuBr and bipyridine, yielding PMPC-, FCP-1-, and FCP-2-grafted substrates. PTDFOMA-grafting was performed similarly, employing a 0.8 M trifluorotoluene (TFT) solution of monomer at 60 °C, with CuBr and 4,4′-dinonyl-2,2′-dipyridyl (dNbpy). Following these grafting methods, the presence of polymer on the substrates was confirmed by X-ray photoelectron spectroscopy (XPS), noting the C, N, O, F, and P in the XPS scan of FCP-2 (**Figure 2a**) at elemental percentages that agreed with theoretical values (C 46.15%, N 2.56%, O 15.38%, F 33.33%, P 2.56%). In the high-resolution C_{1s} spectrum of FCP-2, peak deconvolution revealed distinct carbon atoms (**Figure 2b**) at 284.8 eV (C-C), 286 eV (C-N), 286.7 eV (CH_2-O), 288.6 eV (C=O), 290.4 eV (-CF_2-CF_2-CH_2), 291.4 eV (CF_2), and 293.6 eV (CF_3). Similar scans performed on FCP-1, PMPC, and PTDFOMA-grafted substrates (**Figure S5**)

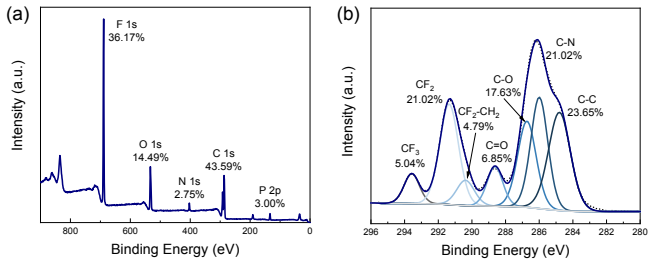

Figure. 2. XPS spectra of **FCP-2**-grafted Au: (a) survey spectrum and (b) C_{1s} scan.

verified the presence of the desired polymers and as such the general utility of SI-ATRP for the selected monomers. Thickness values for the polymer layers were ~40-60 nm (measured by ellipsometry and calculated using the Cauchy model[24]), suggesting considerable extents of grafting and as such the presence of sufficient polymer coverage to modify surface properties and perform comparative evaluations across this set of samples. The grafted polymer chains are considered to be in the brush regime,[25] with grafting densities estimated as 0.12, 0.30, 0.28 and 0.18 chains/nm^2 for PMPC-, FCP-1-, FCP-2- and PTDFOMA-modified surfaces, respectively (see SI for detailed calculation).

Wettability characteristics of the polymer-modified substrates were evaluated by contact angle measurements, using water (in air) and trifluorotoluene (in water) as probe fluids. As shown in **Figure 3a-d** and **Table 1**, the PMPC-functionalized substrates exhibited very small contact angles, typically ~15°, due to the extensive hydrophilicity of this polymer zwitterion. In contrast, the fluorocarbon-rich PTDFOMA-grafted substrates repelled water, yielding contact angles of ~120°. Substrates grafted with fluorinated zwitterions **FCP-1** and **FCP-2** had water contact angles intermediate between these extremes, measuring 69° for **FCP-1** and 85° for **FCP-2**. Thus, the effect of merging zwitterionic and fluorocarbon moieties pendent to the polymer backbone effectively alters the typical wetting properties of each: i.e., fluorocarbon polymers take on appreciable hydrophilicity, while polymer zwitterions gain an unusual degree of hydrophobicity. With respect to film thickness, we observed water contact angles to remain almost unchanged for PMPC and PTDFOMA-modified surfaces irrespective of thickness (~10° for PMPC surfaces at 8.5, 34.3, and 67.2 nm; ~120° for PTDFOMA surfaces at 10.9, 42.2, and 59.6 nm). The FCP polymer series showed minor variability: FCP-1-grafting gave water a contact angle of 55° for 10 nm and ~70° for 30 nm thick films, whereas the FCP-2-grafted surface had a water contact angle of 109° at 8 nm and ~80-90° at 50-70 nm. (**Table S2**). Interestingly, when performing contact angle measurements with TFT in water, the zwitterion-containing substrates repelled the droplet with high contact angles (>140°, **Figure 3e-g**), while the PTDFOMA-grafted surface was wet significantly by TFT (contact angle ~31°).

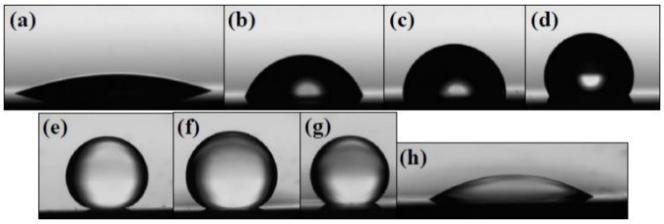

Figure. 3. Photographs from static contact angle measurements of water on grafted substrates: (a) **PMPC**; (b) **FCP-1**; (c) **FCP-2**; and (d) **PTDFOMA**. Similar experiments using TFT as the probe fluid shown in (e) **PMPC**; (f) **FCP-1**; (g) **FCP-2**; and (h) **PTDFOMA**.

Solid-vapor (sv) surface energies (γ_{SV}, the sum of the dispersive (γ_{SV}^d) and polar (γ_{SV}^p) components) were calculated using Young's equation (**Equation 1**) and the Owens-Wendt equation (**Equation 2**), employing the known surface energy (γ_{LV}) of the

$$\gamma_{SV} = \gamma_{SL} + \gamma_{LV}cos\theta \qquad \textbf{Equation 1}$$

$$\gamma_{LV}(1 + cos\theta) = 2(\gamma_{SV}^d\gamma_{LV}^d)^{1/2} + 2(\gamma_{SV}^p\gamma_{LV}^p)^{1/2} \qquad \textbf{Equation 2}$$

test liquids—water, diiodomethane, and glycerol—and measurements of their contact angles (θ) on each surface in air

(**Table S1**). The contact angle values of diiodomethane on the PMPC-, FCP-1-, FCP-2-, and PTDFOMA-modified surfaces in air were measured as 21°, 68°, 72°, and 100°, respectively; a similar trend was seen when using glycerol (38°, 72°, 90°, and 108° on the same series). These data yield surface energies of 70.4, 34.2, 23.4, and 9.3 mJ/m^2 for PMPC-, FCP-1-, FCP-2- and PTDFOMA-modified substrates, respectively, confirming the dominant impact of the fluorine-rich PTDFOMA on surface energy, and the surface energy modulation achieved with the embedded zwitterions. The calculated γ_{SV} and the observed water contact angles and surface/water interfacial energies (γ_{SL}) reported in **Table 1** were determined using **Equation 1**. ThePMPC-grafted substrates exhibited exceptionally low γ_{SL} values 0.3 mJ/m^2, while γ_{SL} values of FCP-1-, FCP-2-, and PTDFOMA- grafted surfaces were calculated to be 7.5, 17.4, and 45.3 mJ/m^2, respectively. The lower γ_{SL} of PMPC-, FCP-1-, and FCP-2-modified surfaces hindered spreading of TFT in water (TFT/water interfacial energy = 33.8 mJ/m^2), resulting in high contact angles, while the PTDFOMA-modified surface showed the expected wettability when probed with TFT.

Table 1. Contact angle and surface energy values of substrates grafted with PMPC, FCP-1, FCP-2, and PTDFOMA. Results represent the average of measurements recorded at three different spots on the substrates.

	PMPC	FCP-1	FCP-2	PTDFOMA
Water, static (°)	**14.8**	**68.5**	**85.3**	**119.6**
Water, advancing (°)	**14.5**	**79.3**	**114.7**	**125.0**
Water, receding (°)	**<10**	**16.7**	**24.7**	**77.2**
TFT in water, static (°)	**160.5**	**154.7**	**142.3**	**30.9**
γ_{SV} (mJ/m^2)	**70.4**	**34.2**	**23.4**	**9.3**
γ_{SL} (mJ/m^2)	**0.3**	**7.5**	**17.4**	**45.3**

The wetting behavior described to this point suggests that the disparate zwitterionic and fluorinated components of FCP-1 and FCP-2 are sensitive to their surrounding environment that suggest *in situ* molecular reorganization. Recent examples of conformational rearrangements of fluorinated polymers have been reported for thin films and grafted brushes of poly(fluoroalkyl acrylate)s, which reorient to present carbonyl groups to the water interface.[26-28] In addition, Wooley reported PEGylated hyperbranched fluoropolymers with domains that reorganize in response to the surrounding liquid, giving nanoscale complexity and non-fouling properties.[29-31] In our work, the fluorinated groups of FCP-1 and FCP-2 strongly prefer the air interface, due to the apolar and self-associating properties of fluoroalkanes. However, when immersed in water, the strongly hydrophilic zwitterionic groups induce segregation to the polymer-water interface, imparting a significant degree of hydrophilicity (fluorophobicity) to substrates modified with FCP-1 and FCP-2.

Our findings are further supported by dynamic water contact angle measurements that recorded large contact angle hysteresis values for surfaces grafted with FCP-1 (~60°) and FCP-2 (~90°) (**Table 1**). In these measurements, increasing the volume of water employed led to repulsion of the droplet (and correspondingly high contact angle) by fluorinated groups at the polymer-air interface (**Figure 4a**). The advancing angles were sensitive to fluorine content, trending as FCP-1 (79°) < FCP-2 (115°) < PTDFOMA (125°). Notably, the low receding angles of FCP-1 (17°) and FCP-2 (25°) are due to the zwitterionic units that prefer the water-polymer interface (**Figure 4b**), which are absent in PTDFOMA (receding angle ~77°). When the substrates were oriented vertically, the drop resisted sliding down the FCP-2 surface but traversed the PTDFOMA surface quickly. Such hydrophobic surfaces that retain water (i.e., exhibit large contact angle hysteresis) mimic the surface wettability of rose petals and are interesting for studies in water transport. Surfaces of this type are typically obtained by manipulation of surface topology,[10,32] but here are achieved using the advantageous FCP design in combination with surface grafting techniques.

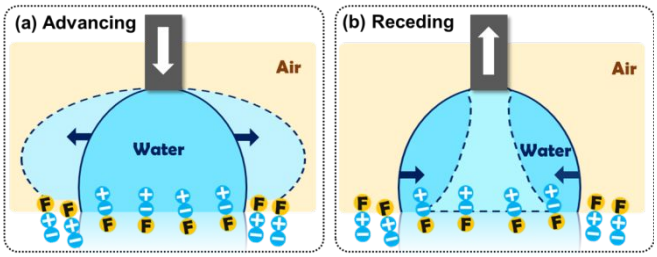

Figure. 4. Schematic illustration of **FCP** reorganization: (a) advancing and (b) receding contact angle measurements.

To examine protein adsorption on these polymer-modified substrates, SPR was employed (using the Biacore T200 system) to assess the change in the angle of minimum reflectivity (SPR angle) as refractive index is altered upon protein adherence or dissociation (**Figure 5a**).[33-37] Based on literature precedent,[38-40] our experimental design equated one response unit change (ΔRU) with 0.1 ng/cm^2 of protein. These experiments were performed by first subjecting the protein solution (1 mg/mL) to the surfaces at a flow rate of 20 µL/min for 300 seconds, then rinsing the surfaces with PBS buffer for 300 seconds at 20 µL/min to remove any loosely adsorbed protein. As seen in **Figure 5b,** all of the polymer-grafted surfaces reduced BSA adsorption considerably relative to bare Au, giving ng/cm^2 values of 228.1 (bare gold), 56.2 (PTDFOMA), 36.8 (PMPC), 17.6 (FCP-2), and 9.5 (FCP-1); after rinsing with PBS, these values were reduced to 204.2, 42.6, 17.9, 3.6 and 0.6 ng/cm^2, respectively. *FCP-1 and FCP-2 exhibited particularly impressive adsorption resistance and foulant release against BSA*, with >75% reduction in BSA content after rinsing. In the lysozyme adsorption study, bare gold, PMPC-, FCP-1-, FCP-2- and PTDFOMA-modified surfaces had adsorption values of 152.3, 54.4, 51.3, 27.5, and 16.9 ng/cm^2 upon applying lysozyme solution, respectively, which reduced to 123.3, 36.9, 37.4, 13.6 and 10.6 ng/cm^2 after rinsing (**Figure S6**). Notably, the inclusion of the perfluorohexyl structure in FCP-2 effectively reduced lysozyme adhesion in comparison to PMPC; in the FCP-2 case, 53% of the adsorbed lysozyme was removed after rinsing, resulting in similar adsorption levels as seen for PTDFOMA-modified surfaces. In general, the combination of fluorinated and zwitterionic structures promotes antifouling properties of

each, by reducing protein adhesion as well as promoting release.

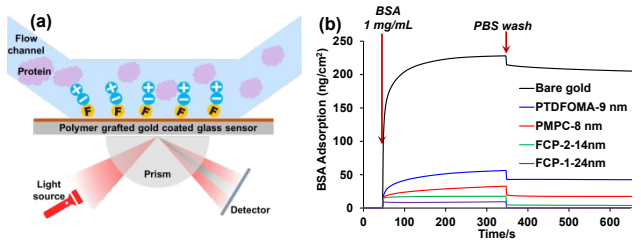

Figure. 5. (a) Schematic illustration of SPR measurements; (b) BSA adsorption on grafted substrates measured by SPR.

Conclusions

In summary, we described the impact of grafting surfaces with fluorinated polymer zwitterions and specifically the unique wettability and anti-fouling attributes of these fluorinated zwitterions relative to conventional polymer zwitterions and polymeric fluorocarbons. The fluorinated zwitterionic polymers, FCP-1 and FCP-2, exhibited hydrophobicity in air and fluorophobicity in water, as well as remarkably high contact angle hysteresis. The observed dynamic wetting behavior suggests a reorganization of fluorinated and zwitterionic units in response to the contacting fluidic environment. Remarkably, FCP-1- and FCP-2-grafted surfaces afforded comparable or better protein resistance than the PMPC- and PTDFOMA-modified surfaces against BSA and lysozyme, suggesting significant future potential of this class of polymers for making advances in surface modification and wetting control.

Conflicts of interest

There are no conflicts to declare.

Acknowledgements

The authors acknowledge support for this work from the Department of Energy, Office of Basic Energy Sciences, Division of Materials Science and Engineering (DE-SC0008876) for the preparation of bioinspired materials and smart interfaces, as well as support from the National Institutes of Health (AR069079 and CA196947) for integration of fluorinated components into water soluble polymers.

Notes and references

1 W. Sun, W. Liu, Z. Wu and H. Chen, *Macromol Rapid Commun*, 2020, **41**, 1900430.
2 W. L. Chen, R. Cordero, H. Tran and C. K. Ober, *Macromolecules*, 2017, **50**, 4089–4113.
3 M. Elizabeth Welch, Y. Xu, H. Chen, N. Smith, M. E. Tague, H. D. Abruña, B. Baird and C. K. Ober, *Journal of Photopolymer Science and Technology*, 2012, **25**, 53–56.
4 Y. Si, Z. Dong and L. Jiang, *ACS Cent Sci*, 2018, **4**, 1102–1112.
5 T. Dong and T. J. McCarthy, *ACS Appl Mater Interfaces*, 2017, **9**, 41126–41130.
6 L. Gao and T. J. McCarthy, *J Am Chem Soc*, 2006, **128**, 9052–9053.
7 A. Bratek-Skicki, V. Cristaudo, J. Savocco, S. Nootens, P. Morsomme, A. Delcorte and C. Dupont-Gillain, *Biomacromolecules*, 2019, **20**, 778–789.
8 A. R. G. Srinivas, R. Hilali, M. Damavandi, J. Malmstrom, D. Barker, E. Weatherall, G. Willmott and J. Travas-Sejdic, *ACS Appl Polym Mater*, 2021, **3**, 279–289.
9 J. Ji, J. Fu and J. Shen, *Advanced Materials*, 2006, **18**, 1441–1444.
10 A. M. Telford, B. S. Hawkett, C. Such and C. Neto, *Chemistry of Materials*, 2013, **25**, 3472–3479.
11 J. N. Pagaduan, N. Hight-Huf, A. Datar, Y. Nagar, M. Barnes, D. Naveh, A. Ramasubramaniam, R. Katsumata and T. Emrick, *ACS Nano*, 2021, **15**, 2762–2770.
12 B. Li, P. Jain, J. Ma, J. K. Smith, Z. Yuan, H.-C. Hung, Y. He, X. Lin, K. Wu, J. Pfaendtner and S. Jiang, *Sci Adv*, 2019, **5**, 9562–9576.
13 A. H. Jesmer, V. Huynh, A. S. T. Marple, X. Ding, J. M. Moran-Mirabal and R. G. Wylie, *ACS Appl Mater Interfaces*, 2021, **13**, 52362–52373.
14 S. Lowe, N. M. O'Brien-Simpson and L. A. Connal, *Polym Chem*, 2014, **6**, 198–212.
15 Z. Chen, *Langmuir*, 2022, **38**, 4483–4489.
16 H. Huang, C. Zhang, R. Crisci, T. Lu, H. C. Hung, M. S. J. Sajib, P. Sarker, J. Ma, T. Wei, S. Jiang and Z. Chen, *J Am Chem Soc*, 2021, **143**, 16786–16795.
17 A. M. C. Maan, A. H. Hofman, W. M. de Vos and M. Kamperman, *Adv Funct Mater*, 2020, **30**, 2000936.
18 A. Wang, S. Duan, Y. Hu, X. Ding and F.-J. Xu, ACS Appl Mater Interfaces, 2022, **14,** 39, 44173-44182.
19 B. Xu, Y. Liu, X. Sun, J. Hu, P. Shi and X. Huang, *ACS Appl Mater Interfaces*, 2017, **9**, 16517–16523.
20 H. X. Wu, X. H. Zhang, L. Huang, L. F. Ma and C. J. Liu, *Langmuir*, 2018, **34**, 11101–11109.
21 H.-X. Wu, L. Tan, M.-Y. Yang, C.-J. Liu and R.-X. Zhuo, *RSC Adv*, 2015, **5**, 12329–12337.
22 L. Zhou, A. Triozzi, M. Figueiredo and T. Emrick, *ACS Macro Lett*, 2021, **10**, 1204–1209.
23 R. R. Shah, D. Merreceyes, M. Husemann, I. Rees, N. L. Abbott, C. J. Hawker and J. L. Hedrick, *Macromolecules*, 2000, **33**, 597–605.
24 H. Xie, J. Wei and X. Zhang, *J Phys Conf Ser*, 2006, **28**, 95.
25 T. Wu, K. Efimenko and J. Genzer, *J Am Chem Soc*, 2002, **124**, 9394–9395.
26 K. Honda, H. Yakabe, T. Koga, S. Sasaki, O. Sakata, H. Otsuka and A. T. Ãy, *Chem Lett*, 2005, **34**, 1024–1025.
27 K. Honda, M. Morita, H. Otsuka and A. Takahara, *Macromolecules*, 2005, **38**, 5699–5705.
28 A. van Dam, M. M. J. Smulders and H. Zuilhof, *Appl Surf Sci*, 2022, **579**, 152264.
29 K. A. Pollack, P. M. Imbesi, J. E. Raymond and K. L. Wooley, *ACS Appl Mater Interfaces*, 2014, **6**, 19265–19274.
30 P. M. Imbesi, J. A. Finlay, N. Aldred, M. J. Eller, S. E. Felder, K. A. Pollack, A. T. Lonnecker, J. E. Raymond, M. E. MacKay, E. A. Schweikert, A. S. Clare, J. A. Callow, M. E. Callow and K. L. Wooley, *Polym Chem*, 2012, **3**, 3121–3131.
31 C. S. Gudipati, C. M. Creenlief, J. A. Johnson, P. Prayoncpan and K. L. Wooley, *J Polym Sci A Polym Chem*, 2004, **42**, 6193–6208.
32 L. Wang, J. Wei and Z. Su, *Langmuir*, 2011, **27**, 15299–15304.
33 X. Zheng, C. Zhang, L. Bai, S. Liu, L. Tan and Y. Wang, *J Mater Chem B*, 2015, **3**, 1921–1930.
34 R. E. Holmlin, X. Chen, R. G. Chapman, S. Takayama and G. M. Whitesides, *Langmuir*, 2001, **17**, 2841–2850.
35 Y. Dang, M. Quan, C. M. Xing, Y. B. Wang and Y. K. Gong, *J Mater Chem B*, 2015, **3**, 2350–2361.

36 L. R. St. Hill, J. W. Craft, P. Chinwangso, H. V. Tran, M. D. Marquez and T. R. Lee, *ACS Appl Bio Mater*, 2021, **4**, 1563–1572.
37 C. M. Xing, F. N. Meng, M. Quan, K. Ding, Y. Dang and Y. K. Gong, *Acta Biomater*, 2017, **59**, 129–138.
38 K. Yoshioka, Y. Sato, M. Tanaka, T. Murakami and O. Niwa, *Anal Sci*, 2010, **26**, 33–37.
39 N. J. de Mol and M. J. E. Fischer, *Surface Plasmon Resonance: Methods and Protocols*, 2010.
40 X. Zheng, C. Zhang, L. Bai, S. Liu, L. Tan and Y. Wang, *J Mater Chem B*, 2015, **3**, 1921–1930.